J Mater Sci (2010) 45:2174–2180
DOI 10.1007/s10853-009-4056-9

HTC2009

The optimum contact angle range for metal foam stabilization: an experimental comparison with the theory

A. J. Klinter · C. A. Leon · R. A. L. Drew

Received: 15 June 2009 / Accepted: 21 November 2009 / Published online: 15 December 2009

Abstract Using the powder metallurgy (PM) route, metal foam precursors were produced from pure aluminum, Al–1 Mg, Al–7Cu, and Al–11.5Si containing 1 wt% TiH_2 as blowing agent and 8 vol% Al_2O_3 as stabilizer. Subsequent foaming of these precursors in an expandometer at 90 and 140 °C above the melting point or the liquidus temperature of the metal produced expansion curves for each metal/Al_2O_3 composition. These expansion curves, as well as foaming experiments (interrupted at maximum expansion as well as 5 min after maximum expansion), were used to judge the stability of the foams produced from the different metal/Al_2O_3 compositions. Foam stability and wetting behavior of the same metal/Al_2O_3 combinations were used to evaluate the validity of contact angle measurements during idealized wetting experiments to be used to predict promising metal/stabilizing ceramic particle combinations for foam production based on the model proposed by Kaptay.

A. J. Klinter (✉)
Department of Mining and Materials Engineering, McGill University, 3610 University Street, Montreal, QC H3A 2B2, Canada
e-mail: andreas.klinter@mail.mcgill.ca

C. A. Leon
Instituto de Investigaciones Metalúrgicas, Universidad Michoacana de San Nicolás de Hidalgo, Apdo. Postal 888, c.p., 58000 Morelia, Michoacan, Mexico

R. A. L. Drew
Faculty of Engineering and Computer Science, Concordia University, 1455 Maisonneuve Blvd, EV 2.169, Montreal, QC H3G 1M8, Canada

Introduction

Due to reasons of process simplicity, capabilities for small lot sizes, as well as the capacity to manufacture near net shape parts, metal foam research has focused mainly on the powder metallurgy (PM) route. In this technique, metal powders (most commonly aluminum powders with small additions of alloying elements) are mixed with a blowing agent (usually TiH_2) and compacted. Subsequent heating of these precursors above the melting point of the metal results in significant expansion of the compact due to pore formation caused by the decomposition of the foaming agent [1].

Particularly in the liquid foaming technique, in which different gases are blown directly into a bath of liquid metal (most commonly aluminum alloys), ceramic particles such as Al_2O_3, SiC, or TiB_2 are added to the molten metal to stabilize the metal foam. Based on an experimental simulation by Sun et al. [2], as well as a theory by Kaptay [3], it is believed that the aluminum alloy melt needs to wet the added ceramic particles in a certain contact angle range. Kaptay [4] developed different models of particle-arrangements (single layer, closely packed double layer, or complex 3-dimensional networks) along the liquid/gas interface. Based on these models, the probability, ε, can be defined that the ceramic particles are stabilized at the liquid/gas interface and that under the same conditions the liquid film separating two bubbles will be stable. The stability of a metal foam while it is liquid is proportional to ε. For a foam with a gas fraction of 50 vol%, Fig. 1 shows ε for a closed packed double layer over the contact angle between liquid metal and ceramic particles. Assuming the actual condition in particle stabilized aluminum foams to be somewhere between the single layer and closely packed double layer models, an optimum

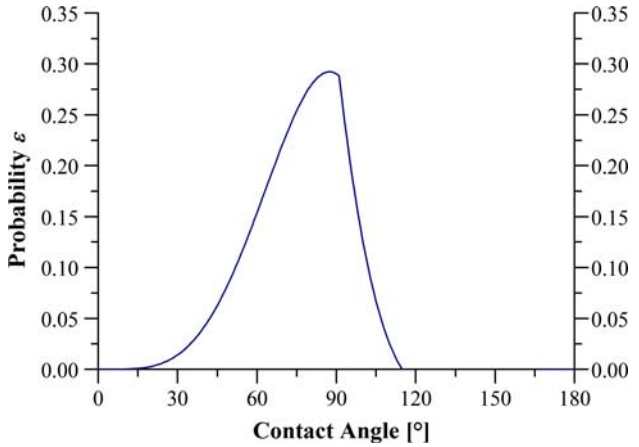

Fig. 1 Probability that ceramic particles are stable at the liquid–gas interface of a foam and that under the same conditions the particles stabilize the bubble against coalescence plotted over the contact angle between liquid and particles

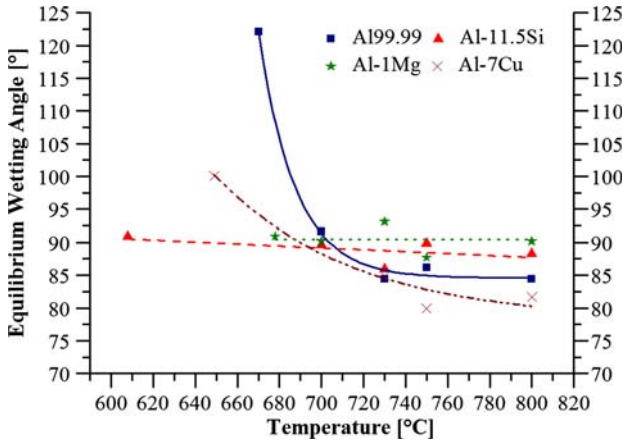

Fig. 2 Wetting behavior of pure aluminum, Al–11.5Si, Al–1Mg, and Al–7Cu on Al_2O_3

contact angle range of the liquid metal on the ceramic particles of 70–86° was derived. Further, following the model, the wetting behavior between liquid and particles becomes essentially irrelevant if complex 3-dimensional networks of particles form at the liquid/gas interfaces of a foam [4]. Ideally, the liquid metal should wet the ceramic particles in the preferred contact angle range over the temperature span between that of the melt bath in the direct foaming method (typically around 750–800 °C [1, 5, 6]) and the solidification temperature of the alloy.

Studies by Kennedy and Asavavisithchai [7, 8] showed that, like in the direct foaming technique, the addition of ceramic particles to the powder mixture from which the precursors are compacted in the PM route to produce aluminum foams can in some cases be beneficial. From particle-stabilized foams presented by other researchers [9–11], it can be seen that the closely packed double layer or complex 3-dimensional network models proposed by Kaptay [4] are the most representative for aluminum foams. Other publications showed that the inherent oxide skin surrounding aluminum powders forms oxide networks inside the cell walls, to which increased foam stability is attributed [12]. Little work, however, has been published on the suspected correlation between wettability and foam stability.

In an earlier publication [13], wetting experiments of pure aluminum and aluminum alloys (Al–1 wt%Mg, Al–7 wt%Cu, and Al–11.5 wt%Si,) on Al_2O_3 were performed under high vacuum in a horizontal tube furnace. The results showed that the Al–Cu alloy on Al_2O_3 exhibits the lowest contact angles (though only at higher temperature), followed by Al–99.99/Al_2O_3, Al–11.5Si/Al_2O_3, and for Al–1Mg/Al_2O_3. For the latter equilibrium contact angles in the non-wetting regime were reported. In contrast to pure aluminum and the Al–Cu alloy, wetting of Al–11.5Si and Al–1Mg on Al_2O_3 behaves independently of temperature (Fig. 2).

Using the PM method, the present work aims to evaluate the possibility to predict foam expansion performance based on wetting behavior and Kaptay's model [4].

Experimental procedure

Powders of −325 mesh (<45 μm) particle size of pure aluminum, pure copper, Al–12Si, and Al–50Mg, as well as high purity Al_2O_3, and TiH_2 (both <5 μm particle size) were used to prepare powder mixtures of pure aluminum, Al–7Cu, Al–1Mg, and Al–11.5Si, each with 1 wt% TiH_2. In order to maintain constant ceramic particle additions, 8 vol% Al_2O_3 was added to the mixtures of metal and blowing agent. In a lubricated die, foamable precursors were subsequently prepared with a diameter of 30 mm and a height of approximately 15 mm using a two stage cold and hot (350 °C) compaction process, which achieved theoretical densities of 90–93% for the Al–7Cu and Al–11.5Si mixtures, and above 98% for the Al–99.99 and Al–1Mg mixtures. Higher hot-compaction temperatures, which would have yielded higher compaction in the cases of the Al–Si and Al–Cu compositions, were not possible as premature decomposition of the blowing agent needed to be avoided.

The foaming experiments were conducted in an expandometer (Fig. 3), the main feature of which is a vertical tube furnace, in which hangs a slightly tapered crucible with a bottom diameter of 31 mm (for ease of sample placement). A thermocouple touches the outside of the crucible wall just above its bottom, and records and controls the foaming temperature. The volume expansion is measured using a laser displacement sensor, as the foam

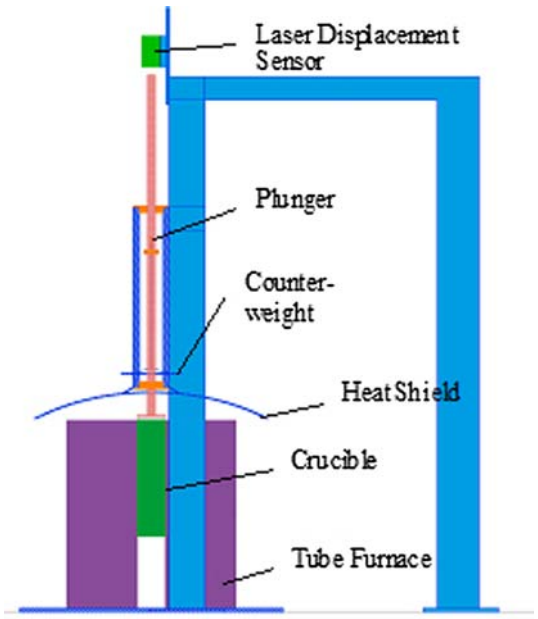

Fig. 3 Schematic of the expandometer used for foaming experiments

expansion is constrained to vertical growth only. A plunger, which is counterweighed to approximately 96% (ratio of counterweight to weight of plunger), is employed to transfer the vertical growth in order to obtain a less noisy signal from the laser sensor, to prevent the typical dome formation at the top of the foam, and to enable the system to measure foam collapse. A heat shield over the top of the tube furnace and crucible prevents excessive heat loss and protects the displacement sensor from thermal damage.

Prior to a foaming experiment, the plunger is fully immersed into the empty crucible. Once the thermocouple shows the experimental temperature without significant fluctuation, a test is conducted by withdrawing the plunger from the crucible, dropping a compact into the latter, and replacing the plunger on top of the compact. A data acquisition system subsequently records expansion from the displacement sensor as well as the crucible/foaming temperature with a 1 Hz frequency.

Foaming experiments were conducted for each powder composition at 90 and 140 °C above the melting point of pure aluminum or the liquidus temperature of the alloys. Expansion curves were recorded over 20 min. Additionally, experiments were interrupted in order to achieve maximum expansion and to determine the foam stability without the load being exerted by the plunger. For these maximum expansion tests, the plunger was retracted when the foaming time at which half of maximum expansion was recorded according to the expansion curves, the crucible was immediately removed from the furnace and cooled to room temperature. Similarly, for the foam stability experiments, the plunger was also withdrawn from the crucible at a time corresponding to half-maximum expansion; however, the crucible with the sample remained in the furnace for another 5 min before it was removed.

Electron microscopy was conducted on several foams after sectioning them along the expansion direction using a Hitachi S4700 field emission gun SEM operating at 2 kV accelerating voltage to avoid charging. Subsequently, the visible pores in each of the foams were spray painted black to obtain better contrast digital photographs. On these, image analysis was conducted using the Clemex Vision software (Professional Edition 5.0) in order to gain more information about pore size distribution, as well as aspect ratio and roundness of pores.

Results and discussion

The liquidus temperatures of the alloys were determined from DSC curves as the temperatures at which the heat flow returns back to the baseline after the melting peak. The values, which were presented earlier, are shown in Table 1. Using the same method, yet using the melting peak itself, the melting point of pure aluminum was verified as 660 °C.

From several of the expansion curves, such as Fig. 4a, b, or e, it can be seen that the expansion onset varies by a few tens of seconds. This is caused by the fact that the placement of the compact into the crucible took slightly longer in the cases with later expansion onset. During these delays, the furnace lost temperature and the hydrogen release onset was consequently delayed.

All compositions at both respective foaming temperatures show a two-stage expansion. In the first, during which the metal just melted, the samples expand in all directions, until the crucible walls are reached. This first expansion stage is also characterized by loss of H_2 to the periphery, since foaming agent decomposition occurs at lower temperature than metal melting. In the second stage, expansion is restricted to a unidirectional growth filling the complete diameter of the crucible and the evolved gas is used more efficiently. As the volume increase to fill the crucible diameter is not considered in the volume growth calculation, the expansion rate in the first stage is always slower. In the cases of the Al–7Cu/Al_2O_3 and Al–11.5Si/Al_2O_3 compositions, a distinct plateau can even be observed between the two stages.

Since the heat input into the sample is greater for the higher of the two respective foaming temperatures,

Table 1 Liquidus temperatures of the alloys [1]

Alloy	Al–99.99	Al–1Mg	Al–7Cu	Al–11.5Si
T_{liq} (°C)	660	658	639	598

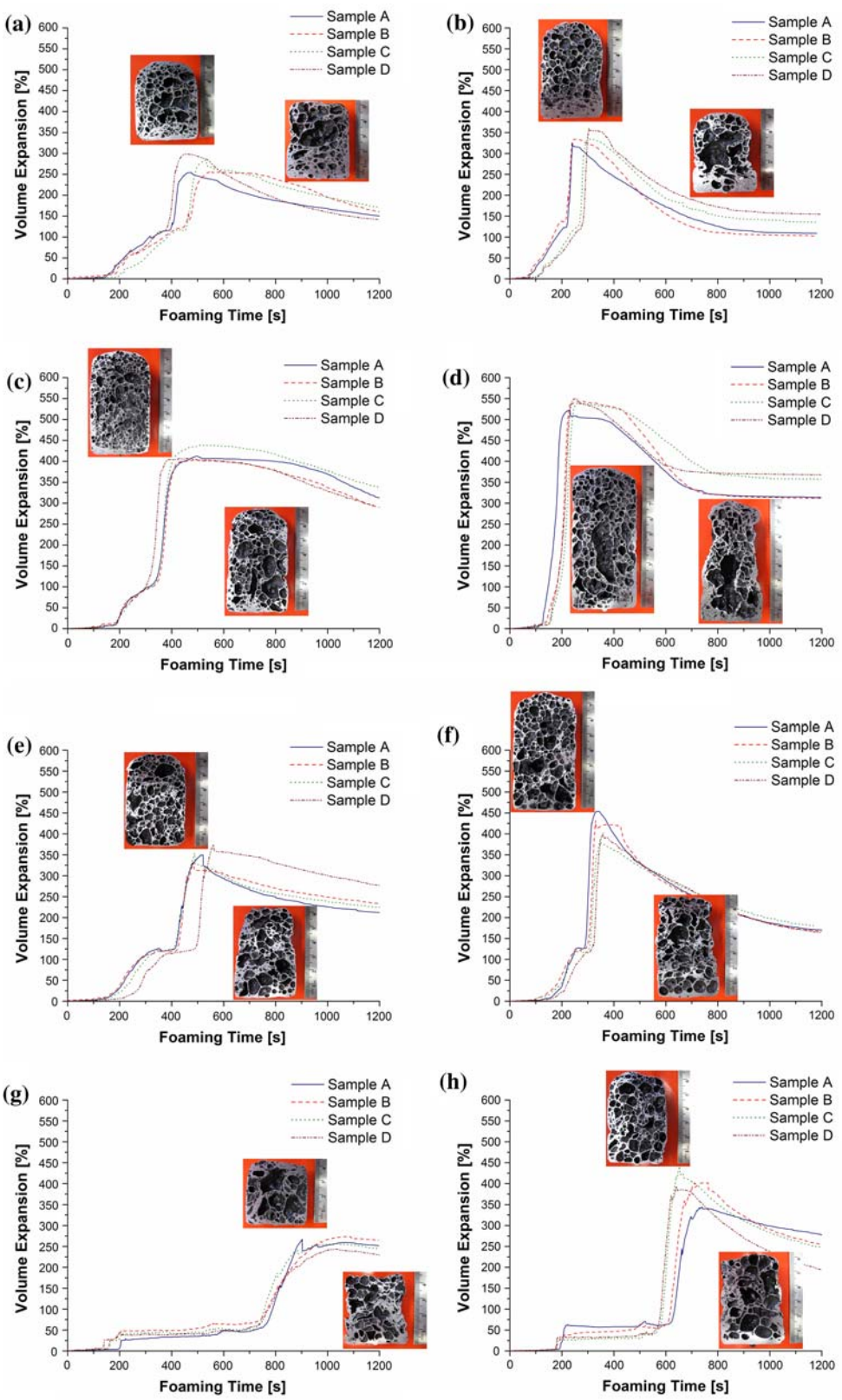

Fig. 4 Foam expansion curves for Al–99.99/Al_2O_3 at 750 °C (**a**) and 800 °C (**b**), Al–1Mg/Al_2O_3 at 748 °C (**c**) and 798 °C (**d**), Al–7Cu/Al_2O_3 at 729 °C (**e**) and 779 °C (**f**), as well as for Al–11.5Si/Al_2O_3 at 688 °C (**g**) and 738 °C (**h**). Inserted in the expansion curves are images cross-sections of the corresponding foams interrupted for maximum expansion as well as the stability tests

the onset of the hydrogen release by the foaming agent and the melting of the alloy are faster at this temperature. This results in less gas being lost through cracks in the compact while it is still solid. Hence, the larger foam expansions are observed for the higher foaming temperatures.

After the maximum expansion has been reached, Al–99.99/Al_2O_3 and Al–7Cu/Al_2O_3 at both respective temperatures, as well as Al–1 Mg/Al_2O_3 and Al–11.5Si/Al_2O_3 at the higher respective foaming temperature, show noticeable foam collapse; the rate and extent of which is higher at the higher foaming temperature. Al–11.5Si/Al_2O_3 at 688 °C and Al–1Mg/Al_2O_3 at 748 °C seem to reach a plateau at maximum expansion. In the case of Al–1Mg, this plateau lasts for approximately 7 min, before collapse can be observed from the expansion curves. During the 20-min foaming experiments at 688 °C, no significant foam collapse is observed for the Al–11.5Si/Al_2O_3 foams. Additional, longer foaming time tests with Al–11.5Si/Al_2O_3, though, show collapse to commence after approximately 23 min (1360 s). Comparing the expansion curves of Al–99.99/Al_2O_3 to the behavior of pure aluminum with 1 wt% TiH_2 but without added ceramic particles [14], one can see that the foams without alumina particles seem to reach slightly higher expansions, however, show noticeably higher foam collapse (Fig. 5).

The foams interrupted to reach maximum expansion generally show more rounded pores and mostly a sharper pore size distribution. Al–11.5Si/Al_2O_3 at 688 °C is an exception in terms of the pore size distribution as it shows a wide range of pore sizes, which appear rather rugged already at maximum expansion. The foams interrupted 5 min after maximum foam expansion all show significant pore coarsening, rather irregular pore shapes, significant drainage of metal to the bottom of the foam, as well as extreme thinning of the cell walls in the upper half of the foam. In the cases of the Al–7Cu/Al_2O_3 foams, some rounded pores usually remain in the bottom third of the foam, surrounded by the drained metal. At the higher of the respective foaming temperatures caving-in of the foam walls is generally apparent in the overaged foams.

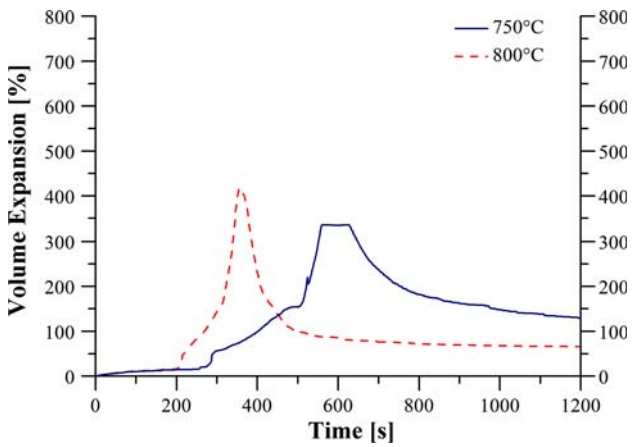

Fig. 5 Foam expansion curves of Al–99.99 with 1 wt% TiH_2 but without ceramic particle addition at 750 and 800 °C after Aguirre-Perales [14]. The compacting procedure in Aguirre-Perales' work is identical to the present one

Al–1Mg/Al_2O_3 foams, particularly at the 798 °C foaming temperature tend to form elongated vertical pores in the center of the foam, which remain somewhat stable even 5 min after maximum expansion.

Assuming the closely packed double layer model (Fig. 1) [4], those liquid metal/solid particle combinations should form the most stable foams that exhibit contact angles in the range of 85°–90°. It is commonly believed that the more stable the foam while the metal is liquid, the more even the foam's pore morphology and the slimmer the pore size distribution. Based on this model and the wetting behavior found previously [13], both Al–11.5Si/Al_2O_3 and Al–1Mg/Al_2O_3 foams should be less stable than pure aluminum/Al_2O_3 and particular Al–7Cu/Al_2O_3 foams, as the latter two reach contact angles that correspond to the highest stability probabilities according to the model (Figs. 1, 2). However, as can be seen from Fig. 4, Al–1Mg/Al_2O_3 foams reach the highest maximum foam expansions among the four different precursor compositions at both temperatures. Moreover, Al–1Mg/Al_2O_3 foams show the best foam stability, and the most advantageous pore morphology, followed by Al–7Cu/Al_2O_3 foams, Al–99.99/Al_2O_3 foams and Al–11.5Si/Al_2O_3 foams. Similarly, Asavavisithchai and Kennedy [7] found a significant improvement in foam stability due to Mg addition to aluminum foams containing Al_2O_3 prepared via the PM route. SEM micrographs of maximum expansion foams of all four compositions are presented in Fig. 6.

As can be seen from these micrographs, better foam stability, quality, and expansion seem to go along with the alumina particles being embedded deeper in the cell walls, as both Al–1Mg/Al_2O_3 and Al–7Cu/Al_2O_3 foams show noticeably smoother cell walls than Al–99.99/Al_2O_3 and Al–11.5Si/Al_2O_3 foams. This, in agreement with Asavavisithchai and Kennedy [7], as well as Kaptay [4], and must be interpreted as improved wetting in the Al–1Mg/Al_2O_3 system than in the Al–99.99/Al_2O_3 system during foaming. However, as such improved wetting behavior has not been observed during the high vacuum wetting experiments shown in [13], it can be understood that the conditions during foaming under standard atmosphere are sufficiently different to cause clearly different wetting behavior. As expected based on the wetting experiments, the most irregular cell walls among the tested systems and hence the least volume expansion and worst foam quality are observed for the Al–11.5Si/Al_2O_3 system.

Thus, based on the contact angle behavior of the tested metal/Al_2O_3 combinations, Kaptay's closely packed double layer model (Fig. 1) predicts the foam stability/quality sequence among these combinations correctly, with exception of Al–1Mg/Al_2O_3, which should yield foams of

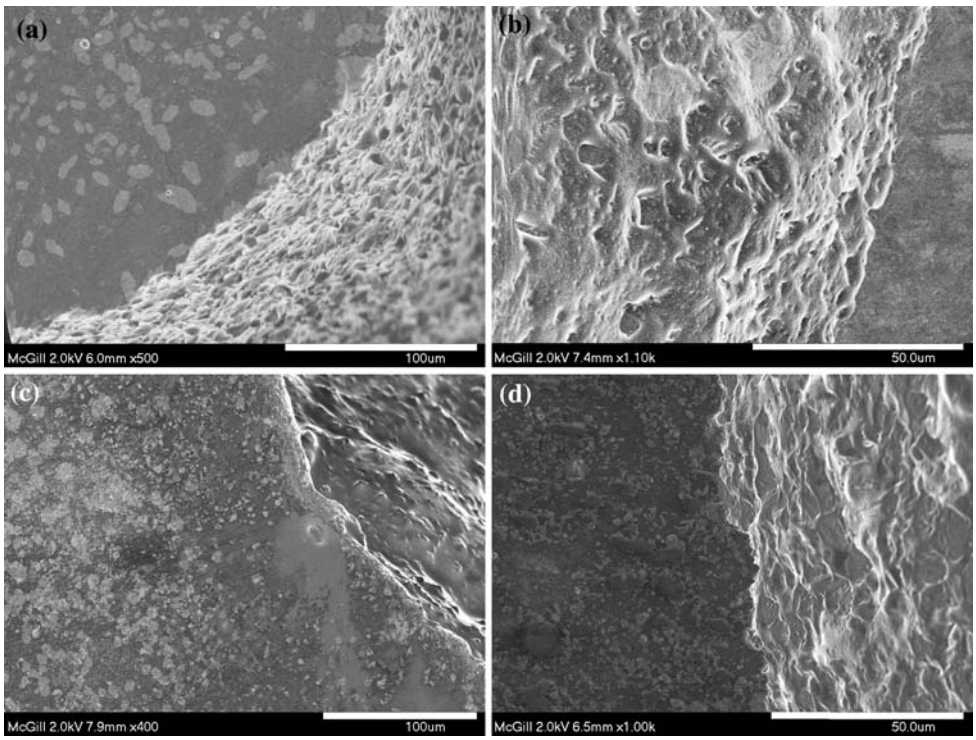

Fig. 6 SEM micrographs of polished sections through an Al–99.99/Al_2O_3 foam (**a**), an Al–1Mg/Al_2O_3 foam (**b**), an Al–7Cu/Al_2O_3 foam (**c**), and an Al–11.5Si/Al_2O_3 foam (**d**), each produced to maximum expansion at the lower respective foaming temperature

similar quality and expansion as Al–11.5Si/Al_2O_3. It can therefore be stated that the model, which has been supported by experimental simulations using aqueous solutions to mimic the liquid metal and polymer or ceramic particles to simulate the ceramic particles [2, 15], is conclusive. Nevertheless, it appears that in the case of aluminum alloy foams containing ceramic particles, wetting experiments under idealized experimental conditions are insufficient to account for the significantly higher oxygen content of the alloys in actual foams (caused by the oxide layers on the metal powder) as well as all reaction processes that occur during foaming. Therefore, such measured contact angles and Kaptay's models can only be a rough guide to which alloy/ceramic particle combinations may be candidates for good foams.

Summary

Using TiH_2 as blowing agent, metal foams were produced via the PM route from metal/Al_2O_3 systems that previously were analyzed for their wetting behavior at relevant temperatures [13]. Foam expansion curves as well as macrostructures of interrupted foaming experiments were employed to evaluate foam quality and stability. Based on these evaluations, it has been found that the model about particle-stabilized metal foams [4], predicting optimum metal foam stability based on measured contact angles between metal and ceramic particles may be used as a general guide to select liquid and stabilizing particles. For aluminum alloy foams stabilized by Al_2O_3 particles, however, it has been shown that additional factors affect foam stability and quality that cannot be grasped during idealized wetting experiments.

Acknowledgements The authors wish to thank the Fonds de Recherche sur la Nature et les Technologies Québec, and the Natural Sciences and Engineering Research Council of Canada for financial support of this project.

References

1. Banhart J (2001) Prog Mater Sci 46:559
2. Sun YQ, Gao T (2002) Metall Mater Trans A Phys Metall Mater Sci 33:3285
3. Kaptay G (1999) In: Banhart J, Ashby MF, Fleck NA (eds) International conference for metal foams and porous metal structures. MIT Press, Bremen, Germany, p 141
4. Kaptay G (2006) Colloids Surf A Physicochem Eng Aspects 282–283:387
5. Jin I, Kenny LD, Sang H (1991) Lightweight foamed metal and its production, at the international patent application. Alcan International Limited, Canada
6. Kenny LD, Thomas M (1994) Process and apparatus for shape casting of particle stabilized metal foam, at the international patent application. Alcan International Limited, Canada
7. Asavavisithchai S, Kennedy AR (2006) Scripta Mater 54:1331
8. Kennedy AR, Asavavisithchai S (2004) Adv Eng Mater 6:400
9. Esmaeelzadeh S, Simchi A, Lehmhus D (2006) Mater Sci Eng A 424:290
10. Haesche M, Weise J, Garcia-Moreno F, Banhart J (2008) Mater Sci Eng A 480:283

11. Körner C (2008) Mater Sci Eng A 495:227
12. Weigand P (1999) PhD Thesis, RWTH Aachen, Aachen
13. Klinter AJ, Mendoza-Suarez G, Drew RAL (2008) Mater Sci Eng A 495:147
14. Aguirre-Perales LY (2010) PhD-Thesis, McGill University, Montreal, Canada (to be published)
15. Nakae H, Kota K (2005) In: Nakajiama H, Kanetake N (eds) International conference on porous metals and metal foaming technology—MetFoam 2005. Japan Institute of Metals, Kyoto, Japan, p 87